Physics Letters B 739 (2014) 44–49

Contents lists available at ScienceDirect

Physics Letters B

www.elsevier.com/locate/physletb

Charge symmetry breaking in $dd \to {}^4\mathrm{He}\pi^0$ with WASA-at-COSY

WASA-at-COSY Collaboration

P. Adlarson [a,1], W. Augustyniak [b], W. Bardan [c], M. Bashkanov [d,e], F.S. Bergmann [f], M. Berłowski [g], H. Bhatt [h], A. Bondar [i,j], M. Büscher [k,l,2,3], H. Calén [a], I. Ciepał [c], H. Clement [d,e], D. Coderre [k,l,m,4], E. Czerwiński [c], K. Demmich [f], E. Doroshkevich [d,e], R. Engels [k,l], A. Erven [n,l], W. Erven [n,l], W. Eyrich [o], P. Fedorets [k,l,p], K. Föhl [q], K. Fransson [a], F. Goldenbaum [k,l], P. Goslawski [f], A. Goswami [k,l,r], K. Grigoryev [k,l,s,5], C.-O. Gullström [a], C. Hanhart [k,l,t], F. Hauenstein [o], L. Heijkenskjöld [a], V. Hejny [k,l,*], B. Höistad [a], N. Hüsken [f], L. Jarczyk [c], T. Johansson [a], B. Kamys [c], G. Kemmerling [n,l], F.A. Khan [k,l], A. Khoukaz [f], D.A. Kirillov [u], S. Kistryn [c], H. Kleines [n,l], B. Kłos [v], W. Krzemień [c], P. Kulessa [w], A. Kupść [a,g], A. Kuzmin [i,j], K. Lalwani [h,6], D. Lersch [k,l], B. Lorentz [k,l], A. Magiera [c], R. Maier [k,l], P. Marciniewski [a], B. Mariański [b], M. Mikirtychiants [k,l,m,s], H.-P. Morsch [b], P. Moskal [c], H. Ohm [k,l], I. Ozerianska [c], E. Perez del Rio [d,e], N.M. Piskunov [u], P. Podkopał [c], D. Prasuhn [k,l], A. Pricking [d,e], D. Pszczel [a,g], K. Pysz [w], A. Pyszniak [a,c], C.F. Redmer [a,1], J. Ritman [k,l,m], A. Roy [r], Z. Rudy [c], S. Sawant [k,l,h], S. Schadmand [k,l], T. Sefzick [k,l], V. Serdyuk [k,l,x], B. Shwartz [i,j], R. Siudak [w], T. Skorodko [d,e], M. Skurzok [c], J. Smyrski [c], V. Sopov [p], R. Stassen [k,l], J. Stepaniak [g], E. Stephan [v], G. Sterzenbach [k,l], H. Stockhorst [k,l], H. Ströher [k,l], A. Szczurek [w], A. Täschner [f], A. Trzciński [b], R. Varma [h], M. Wolke [a], A. Wrońska [c], P. Wüstner [n,l], P. Wurm [k,l], A. Yamamoto [y], L. Yurev [x,7], J. Zabierowski [z], M.J. Zieliński [c], A. Zink [o], J. Złomańczuk [a], P. Żuprański [b], M. Żurek [k,l]

[a] *Division of Nuclear Physics, Department of Physics and Astronomy, Uppsala University, Box 516, 75120 Uppsala, Sweden*
[b] *Department of Nuclear Physics, National Centre for Nuclear Research, ul. Hoza 69, 00-681, Warsaw, Poland*
[c] *Institute of Physics, Jagiellonian University, ul. Reymonta 4, 30-059 Kraków, Poland*
[d] *Physikalisches Institut, Eberhard-Karls-Universität Tübingen, Auf der Morgenstelle 14, 72076 Tübingen, Germany*
[e] *Kepler Center for Astro and Particle Physics, Eberhard Karls University Tübingen, Auf der Morgenstelle 14, 72076 Tübingen, Germany*
[f] *Institut für Kernphysik, Westfälische Wilhelms-Universität Münster, Wilhelm-Klemm-Str. 9, 48149 Münster, Germany*
[g] *High Energy Physics Department, National Centre for Nuclear Research, ul. Hoza 69, 00-681, Warsaw, Poland*
[h] *Department of Physics, Indian Institute of Technology Bombay, Powai, Mumbai, 400076, Maharashtra, India*
[i] *Budker Institute of Nuclear Physics of SB RAS, 11 akademika Lavrentieva prospect, Novosibirsk, 630090, Russia*
[j] *Novosibirsk State University, 2 Pirogova St., Novosibirsk, 630090, Russia*
[k] *Institut für Kernphysik, Forschungszentrum Jülich, 52425 Jülich, Germany*
[l] *Jülich Center for Hadron Physics, Forschungszentrum Jülich, 52425 Jülich, Germany*
[m] *Institut für Experimentalphysik I, Ruhr-Universität Bochum, Universitätsstr. 150, 44780 Bochum, Germany*
[n] *Zentralinstitut für Engineering, Elektronik und Analytik, Forschungszentrum Jülich, 52425 Jülich, Germany*
[o] *Physikalisches Institut, Friedrich-Alexander-Universität Erlangen–Nürnberg, Erwin-Rommel-Str. 1, 91058 Erlangen, Germany*
[p] *Institute for Theoretical and Experimental Physics, State Scientific Center of the Russian Federation, Bolshaya Cheremushkinskaya 25, 117218 Moscow, Russia*

* Corresponding author at: Institut für Kernphysik, Forschungszentrum Jülich, 52425 Jülich, Germany.
E-mail address: v.hejny@fz-juelich.de (V. Hejny).
[1] Present address: Institut für Kernphysik, Johannes Gutenberg-Universität Mainz, Johann-Joachim-Becher Weg 45, 55128 Mainz, Germany.
[2] Present address: Peter Grünberg Institut, PGI-6 Elektronische Eigenschaften, Forschungszentrum Jülich, 52425 Jülich, Germany.
[3] Present address: Institut für Laser- und Plasmaphysik, Heinrich-Heine Universität Düsseldorf, Universitätsstr. 1, 40225 Düsseldorf, Germany.
[4] Present address: Albert Einstein Center for Fundamental Physics, Universität Bern, Sidlerstrasse 5, 3012 Bern, Switzerland.
[5] Present address: III. Physikalisches Institut B, Physikzentrum, RWTH Aachen, 52056 Aachen, Germany.
[6] Present address: Department of Physics and Astrophysics, University of Delhi, Delhi, 110007, India.
[7] Present address: Department of Physics and Astronomy, University of Sheffield, Hounsfield Road, Sheffield, S3 7RH, United Kingdom.

http://dx.doi.org/10.1016/j.physletb.2014.10.029

[q] II. Physikalisches Institut, Justus-Liebig-Universität Gießen, Heinrich-Buff-Ring 16, 35392 Giessen, Germany
[r] Department of Physics, Indian Institute of Technology Indore, Khandwa Road, Indore, 452017, Madhya Pradesh, India
[s] High Energy Physics Division, Petersburg Nuclear Physics Institute, Orlova Rosha 2, Gatchina, Leningrad district 188300, Russia
[t] Institute for Advanced Simulation, Forschungszentrum Jülich, 52425 Jülich, Germany
[u] Veksler and Baldin Laboratory of High Energy Physics, Joint Institute for Nuclear Physics, Joliot-Curie 6, 141980 Dubna, Moscow region, Russia
[v] August Chełkowski Institute of Physics, University of Silesia, Uniwersytecka 4, 40-007, Katowice, Poland
[w] The Henryk Niewodniczański Institute of Nuclear Physics, Polish Academy of Sciences, 152 Radzikowskiego St, 31-342 Kraków, Poland
[x] Dzhelepov Laboratory of Nuclear Problems, Joint Institute for Nuclear Physics, Joliot-Curie 6, 141980 Dubna, Moscow region, Russia
[y] High Energy Accelerator Research Organization KEK, Tsukuba, Ibaraki 305-0801, Japan
[z] Department of Cosmic Ray Physics, National Centre for Nuclear Research, ul. Uniwersytecka 5, 90-950 Łódź, Poland

ARTICLE INFO

Article history:
Received 10 July 2014
Received in revised form 10 September 2014
Accepted 10 October 2014
Available online 16 October 2014
Editor: V. Metag

Keywords:
Charge symmetry breaking
Deuteron–deuteron interactions
Pion production

ABSTRACT

Charge symmetry breaking (CSB) observables are a suitable experimental tool to examine effects induced by quark masses on the nuclear level. Previous high precision data from TRIUMF and IUCF are currently used to develop a consistent description of CSB within the framework of chiral perturbation theory. In this work the experimental studies on the reaction $dd \to {}^4\mathrm{He}\pi^0$ have been extended towards higher excess energies in order to provide information on the contribution of p-waves in the final state. For this, an exclusive measurement has been carried out at a beam momentum of $p_d = 1.2$ GeV/c using the WASA-at-COSY facility. The total cross section amounts to $\sigma_{\mathrm{tot}} = (118 \pm 18_{\mathrm{stat}} \pm 13_{\mathrm{sys}} \pm 8_{\mathrm{ext}})$ pb and first data on the differential cross section are consistent with s-wave pion production.

1. Introduction

Within the Standard Model there are two sources of isospin violation,[8] namely the electro-magnetic interaction and the differences in the masses of the lightest quarks [1,2]. Especially in situations where one is able to disentangle these two sources, the observation of isospin violation in hadronic reactions is a direct window to quark mass ratios [2–4].

The effective field theory for the Standard Model in the MeV range is chiral perturbation theory (ChPT). It maps all symmetries of the Standard Model onto hadronic operators — their strength then needs to be fixed either from experiment or from lattice QCD calculations. At leading order the only parameters are the pion mass and the pion decay constant which are the basis for a series of famous low energy theorems in hadron–hadron scattering (see, for example, Ref. [5]). Although at subleading orders the number of a priori unknown parameters increases, the theory still provides non-trivial links between different operators. A very interesting example is the close link between the quark mass induced proton–neutron mass difference, $\Delta M_{pn}^{\mathrm{qm}}$, and, at leading order, isospin violating πN scattering, the Weinberg term. In general, it is difficult to get access to quark mass effects in low energy hadron physics: by far the largest isospin violating effect is the pion mass difference, which also drives the spectacular energy dependence of the π^0-photoproduction amplitude near threshold (see Ref. [6] and the references therein). Thus, it is important to use observables where the pion mass difference does not contribute. An example is charge symmetry breaking (CSB) observables — charge symmetry is an isospin rotation by 180 degrees that exchanges up and down quarks — as the pion mass term is invariant under this rotation. For this case, the impact of soft photons has been studied systematically [7–11] and can be controlled. Already in 1977 Weinberg predicted a huge effect (up to 30% difference in the scattering lengths for $p\pi^0$ and $n\pi^0$) of CSB in $\pi^0 N$ scattering [1] (see also Ref. [12] for the recent extraction of these quantities from pionic atoms data).

While the $\pi^0 p$ scattering length might be measurable in polarized neutral pion photoproduction very near threshold [13], it is not possible to measure the $n\pi^0$ channel. As an alternative access to CSB pion–nucleon scattering it was suggested in Ref. [14] to use NN induced pion production instead. There have been two successful measurements of corresponding CSB observables, namely a measurement of $A_{fb}(pn \to d\pi^0)$ [15] — the forward–backward asymmetry in $pn \to d\pi^0$ — and of the total cross section of $dd \to {}^4\mathrm{He}\pi^0$ close to the reaction threshold [16].

The first experiment was analyzed using ChPT in Ref. [17] (see also Ref. [18]), where it was demonstrated that $A_{fb}(pn \to d\pi^0)$ is directly proportional to $\Delta M_{pn}^{\mathrm{qm}}$, while the effect of $\pi - \eta$ mixing, previously believed to completely dominate this CSB observable [19], was shown to be subleading. The value for $\Delta M_{pn}^{\mathrm{qm}}$ extracted turned out to be consistent with other, direct calculations of this part based on dispersive analyses [2,20,21] and from lattice. See Ref. [22] for the latest review. In order to cross-check the systematics and to eventually reduce the uncertainties, additional experimental information needs to be analyzed.

The first theoretical results for $dd \to {}^4\mathrm{He}\pi^0$ are presented in [23,24]. The studies show that the relative importance of the various charge symmetry breaking mechanisms is very different compared to $pn \to d\pi^0$. For example, soft photon exchange may significantly enhance the cross sections for $dd \to {}^4\mathrm{He}\pi^0$ [25]. Furthermore, a significant sensitivity of the results to the nuclear potential model was reported in Ref. [26], which called for a simultaneous analysis of CSB in the NN scattering length and in $dd \to {}^4\mathrm{He}\pi^0$ [26]. Thus, as part of a consistent investigation of CSB in the two nucleon sector, $pn \to d\pi^0$ and $dd \to {}^4\mathrm{He}\pi^0$ should help to further constrain the relevant CSB mechanisms.

The main challenge in the calculation of $dd \to {}^4\mathrm{He}\pi^0$ is to get theoretical control over the initial state interactions: high accuracy wave functions are needed for $dd \to 4N$ in low partial waves at relatively high energies. One prerequisite to control this is the earlier WASA-at-COSY measurement of $dd \to {}^3\mathrm{He}n\pi^0$ [27], which is allowed by charge symmetry and partially shares the same initial state as $dd \to {}^4\mathrm{He}\pi^0$. In addition, higher partial waves are predicted to be very sensitive to the CSB $NN \to N\Delta$ transition potential that is difficult to access in other reactions. In leading order in chiral perturbation theory this potential is known.

[8] Ignoring tiny effects induced by the electro-weak sector.

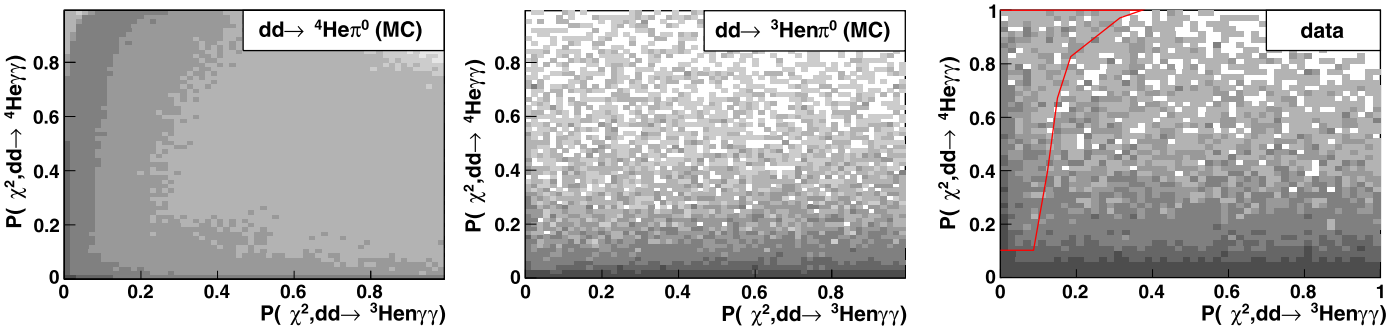

Fig. 1. Cumulative probability distributions from the kinematic fit used for event selection plotted as probability for the ^{4}He hypothesis versus the probability for the ^{3}He hypothesis. Left: distribution for Monte-Carlo simulated signal events for $dd \to {}^4\mathrm{He}\pi^0$, middle: distribution for Monte-Carlo simulated events for $dd \to {}^3\mathrm{He}n\pi^0$, right: distribution for data and the applied probability cut.

Thus, a measurement of, for example, p-waves provides an additional, non-trivial test of our current understanding of isospin violation in hadronic systems. Future theoretical CSB studies for $dd \to {}^4\mathrm{He}\pi^0$ can be based on recent developments in effective field theories for few-nucleon systems [28] as well as for the reaction $NN \to NN\pi$ [29–31], thus promising a model-independent analysis of the data.

While the previous measurements of $dd \to {}^4\mathrm{He}\pi^0$ close to reaction threshold were limited to the total cross section [16], in order to extract constraints on higher partial waves any new measurement at higher excess energies in addition has to provide information on the differential cross section. For this, an exclusive measurement detecting the ^{4}He ejectile as well as the two decay photons of the π^0 has been carried out utilizing the same setup used for $dd \to {}^3\mathrm{He}n\pi^0$ [27]. The latter reaction was also used for normalization.

2. Experiment

The experiment was carried out at the Institute for Nuclear Physics of the Forschungszentrum Jülich in Germany using the Cooler Synchrotron COSY [32] together with the WASA detection system [33]. For the measurement of $dd \to {}^4\mathrm{He}\pi^0$ at an excess energy of $Q \approx 60$ MeV a deuteron beam with a momentum of 1.2 GeV/c was scattered on frozen deuterium pellets provided by an internal pellet target. The ^{4}He ejectile and the two photons from the π^0 decay were detected by the Forward Detector and the Central Detector of the WASA facility, respectively. The experimental setup and trigger conditions were the same as described in Ref. [27].

3. Data analysis

The basic analysis leading to event samples with one helium and two photons in final state follows the strategy used for $dd \to {}^3\mathrm{He}n\pi^0$ outlined in Ref. [27]. Compared to this reaction, however, the charge symmetry breaking reaction $dd \to {}^4\mathrm{He}\pi^0$ has a more than four orders of magnitude smaller cross section. The only other channel with ^{4}He and two photons in final state is the double radiative capture reaction $dd \to {}^4\mathrm{He}\gamma\gamma$. The cross sections for both reactions are not large enough to provide a visual signature for ^{4}He in the previously used ΔE–ΔE plots from the Forward Detector. Thus, all ^{3}He and ^{4}He candidates together with the two photons have been tested against the hypotheses $dd \to {}^4\mathrm{He}\gamma\gamma$ ("^{4}He hypothesis") and $dd \to {}^3\mathrm{He}n\gamma\gamma$ ("^{3}He hypothesis") by means of a kinematic fit. Besides the overall energy and momentum conservation no other constraints have been included. Especially, there is no constraint on the invariant mass of the two photons in order to leave a decisive missing-mass plot and not to introduce a fake $^4\mathrm{He}\pi^0$ signal.

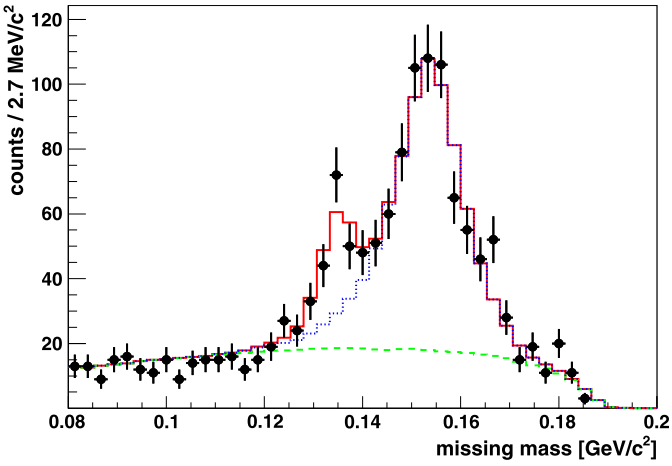

Fig. 2. Missing mass plot for the reaction $dd \to {}^4\mathrm{He}X$. The different contributions fitted to the spectrum are double radiative capture $dd \to {}^4\mathrm{He}\gamma\gamma$ (green dashed), the reaction $dd \to {}^3\mathrm{He}n\pi^0$ (blue dotted, added) and the sum of all contributions including the signal (red solid).

For final event classification the cumulative probabilities $P(\chi^2, n.d.f.)$ for the two hypotheses have been plotted as probability for the ^{4}He hypothesis versus the probability for the ^{3}He hypothesis (see Fig. 1). The data (right plot) have been compared to Monte-Carlo generated samples of $dd \to {}^4\mathrm{He}\pi^0$ events (left plot) and $dd \to {}^3\mathrm{He}n\pi^0$ events (middle plot). Events originating from $dd \to {}^4\mathrm{He}\pi^0$ populate the low probability region for the ^{3}He hypothesis and form a uniform distribution for the ^{4}He hypothesis. As there is no pion constraint in the fit, events from the double radiative capture reaction show the same signature. For $dd \to {}^3\mathrm{He}n\pi^0$ the situation is opposite. The indicated cut is based on the Monte-Carlo simulations, but has been optimized by maximizing the statistical significance of the π^0 signal in final missing mass plot. In addition, it has been checked that the result is stable within the statistical errors against variations of the probability cut. For the simulations the standard Geant3 [34] based WASA Monte-Carlo package has been used, which includes the full detector setup and which has already been benchmarked against a wide range of reactions from the WASA-at-COSY physics program. After this analysis step the contribution from misidentified ^{3}He was reduced by about four orders of magnitude.

In a next step, the resulting four momenta based on the fit hypothesis $dd \to {}^4\mathrm{He}\gamma\gamma$ have been used to calculate the missing mass m_X in $dd \to {}^4\mathrm{He}X$ as a function of the center-of-mass scattering angle θ^* of the particle X. Fig. 2 shows a peak at the pion

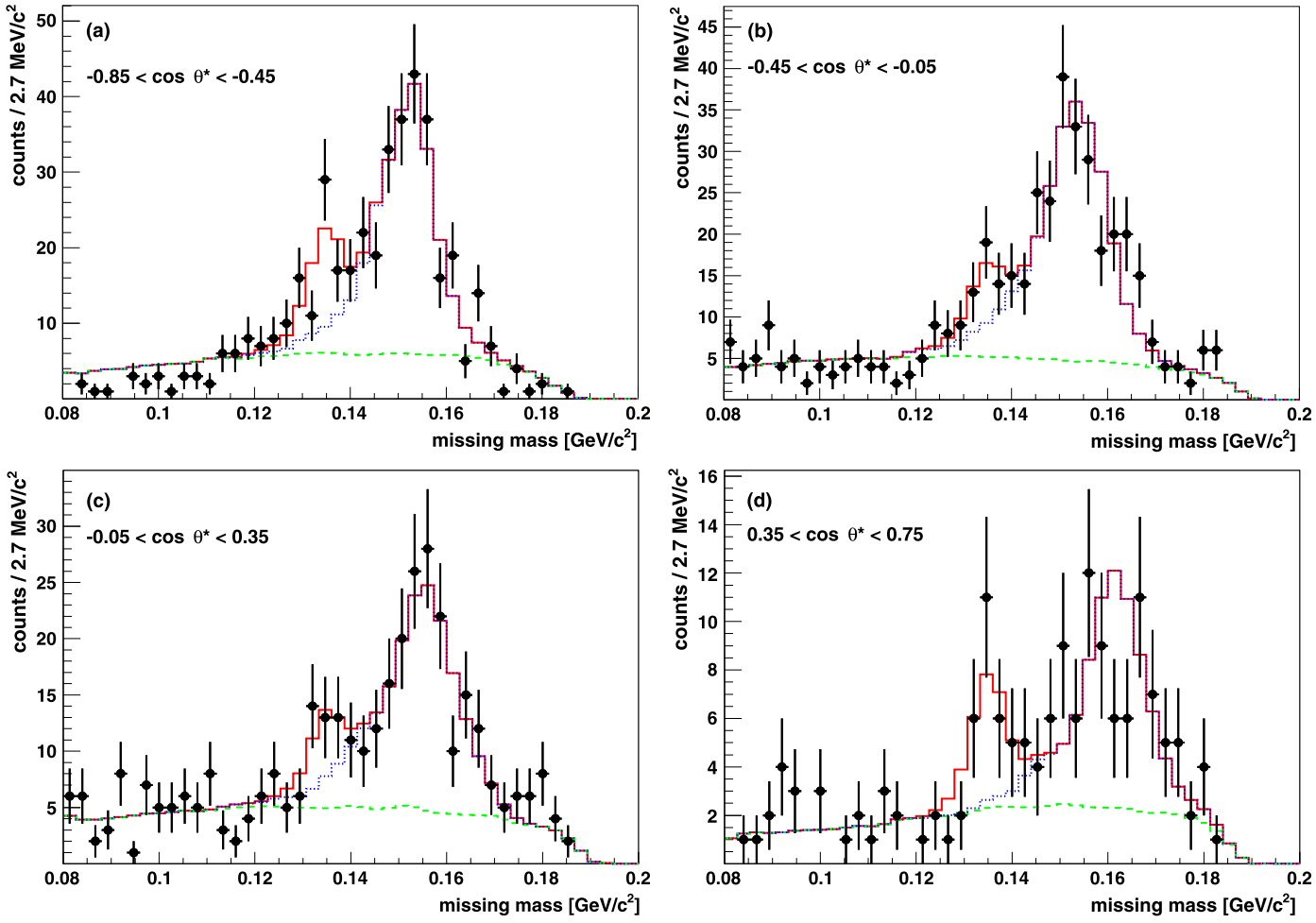

Fig. 3. Missing mass plots for the four different angular bins (scattering angle of the pion in the c.m. system). The color code for the individual contributions is the same as in Fig. 2.

mass on top of a broad background. In order to extract the number of signal events the background in the peak region has to be described and subtracted. Instead of a (rather arbitrary) fit using a polynomial, the shape of signal and background has been reproduced using a composition of physics reactions with a double charged nucleus and two photons in the final state. Any further sources of background — physics as well as instrumental — have already been eliminated by the analysis steps described in Ref. [27] and the subsequent kinematic fit. The signal has then been extracted by fitting a linear combination of the corresponding Monte-Carlo generated high-statistics template distributions for the three reactions

- $dd \to {}^4\mathrm{He}\gamma\gamma$ (double radiative capture) using 3-body phase space (green dashed), plus
- $dd \to {}^3\mathrm{He}n\pi^0$ using the model described in Ref. [27] (blue dotted) for which the ^{3}He is falsely identified as ^{4}He, plus
- $dd \to {}^4\mathrm{He}\pi^0$ using 2-body phase space (*i.e.* plain *s*-wave, red solid).

Please note that in Fig. 2 as well as in Fig. 3 the cumulated distributions are shown, *e.g.* the red solid curve represents the sum of all contributions.

For the differential cross section the data have been divided into four angular bins within the detector acceptance ($-0.85 \leq \cos\theta^* \leq 0.75$). Independent fits of the different contributions listed above have been performed for each bin to address possible anisotropies. In the course of the fit two systematic effects have been observed, which are discussed in the following.

First, the background originating from misidentified ^{3}He is slightly shifted compared to the Monte-Carlo simulations. The effect is angular dependent and is largest at forward angles. Possible reasons are a mismatch in the actual beam momentum, a different amount of insensitive material in Monte-Carlo simulations compared to the real experiment or systematic differences in the simulated detector response for ^{3}He and ^{4}He — the limited statistics did not allow for a detailed study of the origin of that effect. The background stemming from $dd \to {}^3\mathrm{He}n\pi^0$ is sensitive to these effects as the energy losses from a (true) ^{3}He ejectile are used for energy reconstruction of a (falsely identified) ^{4}He. The mismatch can be compensated by introducing an angular dependent scaling factor on the missing mass axis for the $dd \to {}^3\mathrm{He}n\pi^0$ background, which has been included in the fit as additional free parameter. For the angular bins from backward to forward these factors are 1.0, 0.99, 0.97 and 0.94, respectively. As the resulting fits describe the shape of the data especially in the region of the pion peak, no additional systematic error has been assigned to this effect.

The second systematic effect concerns a mismatch in the low mass range $m \leq 0.11$ GeV/c^2 in the most backward angular bin. According to the fit only events from the reaction $dd \to {}^4\mathrm{He}\gamma\gamma$ contribute in this mass region. The model used for this channel was 3-body phase space, which was not expected to provide a perfect description. However, with the dominating background from

$dd \to {}^3\mathrm{He}n\pi^0$ in a wide mass range, it is currently not possible to disentangle the two contributions precisely enough in order to verify any more advanced theoretical model — this issue will be addressed in a follow-up experiment, see below. Consequently, the final fit excludes the corresponding missing mass range (consistently in all angular bins). Based on the difference to the fit with the low mass region included a corresponding systematic uncertainty for this effect has been assigned in the result.

Fig. 3 shows the fitted missing mass spectra for the different bins in $\cos\theta^*$ together with the fit result. The chosen ansatz provides a good overall description of the full data set. Any tests for further systematic effects (according to the definition in Ref. [35]), for example concerning rate effects and selection cuts in the basic analysis (see Ref. [27]), did not reveal any additional systematic uncertainties.

4. Results

For the acceptance correction an isotropic angular distribution has been assumed. For absolute normalization the reaction $dd \to {}^3\mathrm{He}n\pi^0$ has been used. The resulting differential cross sections extracted from Fig. 3 are

$$\frac{\mathrm{d}\sigma}{\mathrm{d}\Omega}\left(-0.85 \leq \cos\theta^* \leq -0.45\right) = (17.1 \pm 3.8 \pm 4.0_{\mathrm{fit}})\ \mathrm{pb/sr}, \quad (1)$$

$$\frac{\mathrm{d}\sigma}{\mathrm{d}\Omega}\left(-0.45 \leq \cos\theta^* \leq -0.05\right) = (6.6 \pm 2.4)\ \mathrm{pb/sr}, \quad (2)$$

$$\frac{\mathrm{d}\sigma}{\mathrm{d}\Omega}\left(-0.05 \leq \cos\theta^* \leq 0.35\right) = (5.5 \pm 2.2)\ \mathrm{pb/sr}, \quad \text{and} \quad (3)$$

$$\frac{\mathrm{d}\sigma}{\mathrm{d}\Omega}\left(0.35 \leq \cos\theta^* \leq 0.75\right) = (8.4 \pm 2.8)\ \mathrm{pb/sr}. \quad (4)$$

In general, only statistical errors are given, except for the first bin where the uncertainty caused by the systematic effect in the low mass region has been included. A systematic error of 10% for luminosity determination and 7% for the normalization to external data is common to all numbers. Integrating the individual results, the (partial) total cross section within the detector acceptance amounts to

$$\sigma_{\mathrm{tot}}^{\mathrm{acc}} = (94 \pm 14_{\mathrm{stat}} \pm 10_{\mathrm{sys}} \pm 6_{\mathrm{ext}})\ \mathrm{pb} \quad (5)$$

with the systematic error originating from luminosity determination and the uncertainty from the different fit methods. The external normalization error has been propagated from the luminosity determination for $dd \to {}^3\mathrm{He}n\pi^0$ (see Ref. [27]). Extrapolation to the full phase space by assuming an isotropic distribution yields

$$\sigma_{\mathrm{tot}} = (118 \pm 18_{\mathrm{stat}} \pm 13_{\mathrm{sys}} \pm 8_{\mathrm{ext}})\ \mathrm{pb}. \quad (6)$$

This result can be compared with the values measured close to threshold by dividing out phase space (see Fig. 4). A constant value could be interpreted as a dominating s-wave, but one has to keep in mind that the energy dependence of the formation of a ^{4}He in the $4N$ final state might have some influence here, too.

Fig. 5 shows the differential cross section. Due to the identical particles in the initial state, odd and even partial waves do not interfere and the angular distribution is symmetric with respect to $\cos\theta^* = 0$. As the p-wave and s–d interference terms contribute to the quadratic term and the p-wave also adds to the constant term, the different partial waves cannot be directly disentangled. However, a fit including the Legendre polynomials $P_0(\cos\theta^*)$ and $P_2(\cos\theta^*)$ — although not excluding — does not show any evidence for contributions of higher partial waves:

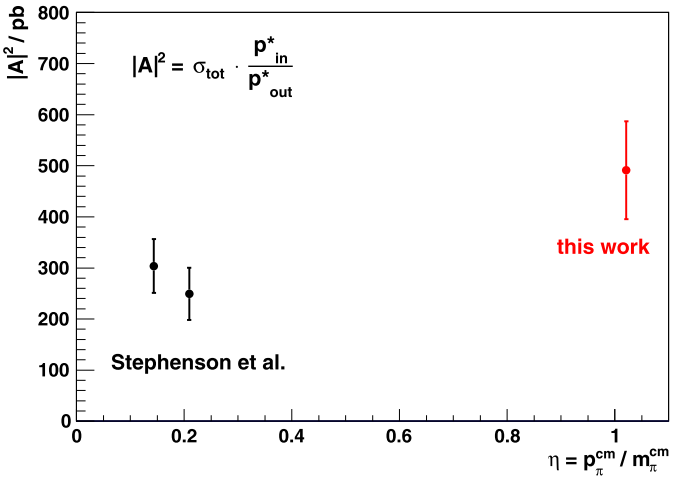

Fig. 4. Energy dependence of the reaction amplitude squared $|A|^2$. In the absence of initial and final state interactions a constant amplitude would indicate that only s-wave is contributing. The red full circle corresponds to the total cross section given in the text. (For interpretation of the references to color in this figure legend, the reader is referred to the web version of this article.)

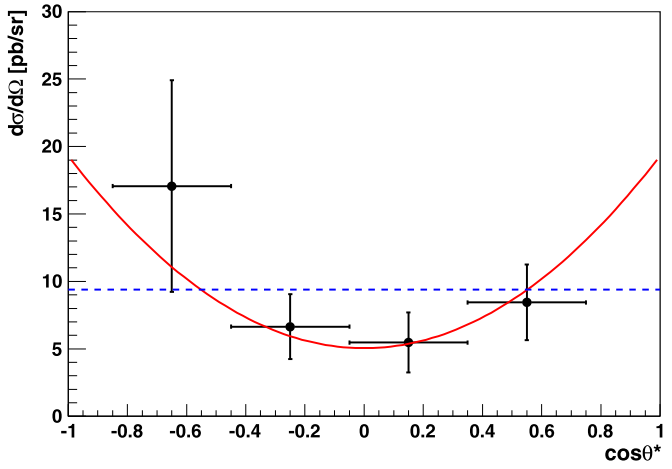

Fig. 5. Differential cross section. The errors bars show the statistical uncertainties. In the first bin the additional systematic uncertainty from the fit has been added (see text). The blue dashed line represents the total cross section given in the text assuming an isotropic distribution, the solid red curve shows the fit with the Legendre polynomials P_0 and P_2.

$$\frac{\mathrm{d}\sigma}{\mathrm{d}\Omega} = (9.8 \pm 2.6)\ \mathrm{pb/sr} \cdot P_0\left(\cos\theta^*\right) + (9.5 \pm 7.4)\ \mathrm{pb/sr} \cdot P_2\left(\cos\theta^*\right). \quad (7)$$

Here, the two coefficients are strongly correlated with the correlation parameter 0.85, *i.e.* the reader should not interpret the two contributions as independent results.

Based on the fit results a first estimate of the total cross section of $dd \to {}^4\mathrm{He}\gamma\gamma$ has been extracted assuming a homogeneous 3-body phase space. It amounts to

$$\sigma_{\mathrm{tot}} = (0.92 \pm 0.07_{\mathrm{stat}} \pm 0.10_{\mathrm{sys}} \pm 0.07_{\mathrm{norm}})\ \mathrm{nb}. \quad (8)$$

It should be noted that this result depends on the underlying models for the reactions $dd \to {}^3\mathrm{He}n\pi^0$ and $dd \to {}^4\mathrm{He}\gamma\gamma$. This model dependence is not included in the given systematic error.

5. Summary and conclusions

In this letter results were presented for a measurement of the charge symmetry breaking reaction $dd \to {}^4\mathrm{He}\pi^0$ at an excess

energy of 60 MeV. The energy dependence of the square of the production amplitude might indicate the on-set of higher partial waves or some unusual energy dependence of the s-wave amplitude — given the current statistical error, no conclusion on the strength of the higher partial waves is possible from the differential cross section.

However, since within chiral perturbation theory the leading and next-to-leading p-wave contribution does not introduce any new free parameter (it is expected to be dominated by the Delta-isobar), the data on the strength of higher partial waves presented in this work will still provide a non-trivial constraint for future theoretical analyses.

The results presented here are based on a two-week run using the standard WASA-at-COSY setup. Based on the experiences gained during this experiment another 8 week measurement with a modified detector setup optimized for a time-of-flight measurement of the forward going ejectiles has been performed recently. In total, an increase of statistics by nearly a factor of 10 and significantly reduced systematic uncertainties can be expected. In particular, the experiment has been designed to provide a better discrimination of background events from $dd \to {}^3\mathrm{He}n\pi^0$.

Acknowledgements

We would like to thank the technical and administrative staff at the Forschungszentrum Jülich, especially at the COoler SYnchrotron COSY and at the participating institutes. This work has been supported in part by the German Federal Ministry of Education and Research (BMBF), the Polish Ministry of Science and Higher Education (grant Nos. N N202 078135 and N N202 285938), the Polish National Science Center (grant No. 2011/01/B/ST2/00431), the Foundation For Polish Science (MPD), Forschungszentrum Jülich (COSY-FFE) and the European Union Seventh Framework Programme (FP7/2007–2013) under grant agreement No. 283286.

References

[1] S. Weinberg, Trans. N. Y. Acad. Sci. 38 (1977) 185–201.
[2] J. Gasser, H. Leutwyler, Phys. Rep. 87 (1982) 77–169.
[3] G. Miller, B. Nefkens, I. Šlaus, Phys. Rep. 194 (1990) 1–116.
[4] H. Leutwyler, Phys. Lett. B 378 (1996) 313–318.
[5] S. Weinberg, Phys. Rev. Lett. 17 (1966) 616–621.
[6] V. Bernard, B. Kubis, U.-G. Meißner, Eur. Phys. J. A 25 (2005) 419–425.
[7] U.-G. Meißner, S. Steininger, Phys. Lett. B 419 (1998) 403–411.
[8] G. Müller, U.-G. Meißner, Nucl. Phys. B 556 (1999) 265–291.
[9] N. Fettes, U.-G. Meißner, Phys. Rev. C 63 (2001) 045201.
[10] M. Hoferichter, B. Kubis, U.-G. Meißner, Phys. Lett. B 678 (2009) 65.
[11] J. Gasser, et al., Eur. Phys. J. C 26 (2002) 13–34.
[12] V. Baru, et al., Phys. Lett. B 694 (2011) 473–477;
V. Baru, et al., Nucl. Phys. A 872 (2011) 69–116.
[13] A. Bernstein, Phys. Lett. B 442 (1998) 20–27.
[14] U. van Kolck, J. Niskanen, G. Miller, Phys. Lett. B 493 (2000) 65–72.
[15] A. Opper, et al., Phys. Rev. Lett. 91 (2003) 212302.
[16] E. Stephenson, et al., Phys. Rev. Lett. 91 (2003) 142302.
[17] A. Filin, et al., Phys. Lett. B 681 (2009) 423–427.
[18] D.R. Bolton, G.A. Miller, Phys. Rev. C 81 (2010) 014001.
[19] J.A. Niskanen, Few-Body Syst. 26 (1999) 241–249.
[20] W. Cottingham, Ann. Phys. (N. Y.) 25 (1963) 424–432.
[21] A. Walker-Loud, C.E. Carlson, G.A. Miller, Phys. Rev. Lett. 108 (2012) 232301.
[22] A. Walker-Loud, PoS LATTICE 2013 (2014) 013.
[23] A. Gårdestig, et al., Phys. Rev. C 69 (2004) 044606.
[24] A. Nogga, et al., Phys. Lett. B 639 (2006) 465–470.
[25] T. Lähde, G. Miller, Phys. Rev. C 75 (2007) 055204.
[26] A.C. Fonseca, R. Machleidt, G.A. Miller, Phys. Rev. C 80 (2009) 027001.
[27] P. Adlarson, et al., WASA-at-COSY Collaboration, Phys. Rev. C 88 (2013) 014004.
[28] E. Epelbaum, H.-W. Hammer, U.-G. Meißner, Rev. Mod. Phys. 81 (2009) 1773.
[29] A.A. Filin, et al., Phys. Rev. C 85 (2012) 054001.
[30] A.A. Filin, et al., Phys. Rev. C 88 (2013) 064003.
[31] V. Baru, C. Hanhart, F. Myhrer, Int. J. Mod. Phys. E 23 (2014) 1430004.
[32] R. Maier, et al., Nucl. Phys. A 626 (1997) 395c.
[33] H.H. Adam, et al., WASA-at-COSY Collaboration, arXiv:nucl-ex/0411038, 2004.
[34] GEANT - detector description and simulation tool, CERN Program Library Long Writeup W5013.
[35] R. Barlow, arXiv:hep-ex/0207026, 2002.